ISSN 1541-308X, Physics of Wave Phenomena, 2017, Vol. 25, No. 3, pp. 170–174. © Allerton Press, Inc., 2017.

SPECTROSCOPY OF PHOTONIC CRYSTALS

Coupled Optical Tamm States at Edges of a Photonic Crystal Enclosed by a Composite of Core-Shell Nanoparticles

S. Ya. Vetrov[1,2*], P. S. Pankin[1,3], and I. V. Timofeev[2,3***]**

[1] *Institute of Engineering Physics and Radio Electronics, Siberian Federal University, pr. Svobodny 79, Krasnoyarsk, 660041 Russia*

[2] *Kirensky Institute of Physics, Federal Research Center KSC Siberian Branch Russian Academy of Sciences, Akademgorodok 50, str. 38, Krasnoyarsk, 660036 Russia*

[3] *Laboratory of Nonlinear Optics and Spectroscopy, Siberian Federal University, pr. Svobodny 79, Krasnoyarsk, 660041 Russia*

Received July 19, 2016

Abstract—Coupled optical Tamm states localized at the edges of a photonic crystal enclosed with a nanocomposite are theoretically studied. The nanocomposite consists of nanoparticles with a dielectric core and a metal shell, which are dispersed in a transparent matrix. It is shown that the positions of the spectral peaks are sensitive to the thickness of the outermost photonic crystal layer.

DOI: 10.3103/S1541308X17030025

1. INTRODUCTION

Recently, extensive investigation has been given to a special type of localized electromagnetic states (optical Tamm states (OTSs)) that can be excited by light normally incident on the sample [1, 2]. These states are an analogue of the Tamm surface state in solid state physics. The OTS can be excited between two different photonic crystals (PCs) that have overlapping bandgaps (BGs) [3] or between a PC and a medium with negative permittivity ε (plasma-like medium) [4, 5]. The surface electromagnetic wave at the interface of the PC and the medium with $\varepsilon < 0$ is an inseparable whole with the surface plasmon—oscillations of free electrons near the conductor surface. This coupled mode of the radiation field and the surface plasmon excitation is termed the Tamm plasmon polariton (TPP). The OTS experimentally manifests itself as a narrow peak in the sample transmission spectrum [6, 7].

Potential applications of surface modes and OTSs are sensors and optical switches [8], multichannel filters [9], Faraday rotation amplifiers, Kerr effect amplifiers [10], organic solar cells [11], and absorbers [12].

When the PC is bounded on both sides by a plasma-like medium, coupled TPPs can be obtained [13]. In [5] it was shown that coupled TPP could be obtained using a metal–dielectric nanocomposite (NC) as a plasma-like medium. The position of the frequency interval in which the NC is similar to metal, i.e., where $\mathrm{Re}(\varepsilon(\omega)) < 0$, depends on the permittivity of the NC materials and the concentration and shape of its filling nanoparticles. This opens up wide possibilities of controlling optical properties of OTSs by varying NC parameters.

In this work we investigate the effect of the structure parameters on the spectral manifestation of the coupled TPPs occurring in a PC bounded on both sides by an NC consisting of core-shell particles. The spectral properties of the PC are calculated using the transfer matrix method.

2. MODEL

The PC used consisted of alternating silicon dioxide (SiO_2) and zirconium dioxide (ZiO_2) layers with the respective permittivities and thicknesses $\varepsilon_a = 2.10$, $W_a = 74$ nm and $\varepsilon_b = 4.16$, $W_b = 50$ nm. The PC was bounded on two sides by an NC layer with the thickness $W_d = 150$ nm, which consisted of core-shell layered spherical nanoparticles uniformly distributed in a dielectric matrix of transparent optical glass with the permittivity $\varepsilon_m = 2.56$. The structure consisted of $N = 17$ layers, including NC layers, and was placed in a medium (air) with the permittivity of unity (Fig. 1(a)).

*E-mail: s.vetrov@inbox.ru
**E-mail: ppankin@sfu-kras.ru
***E-mail: tiv@iph.krasn.ru

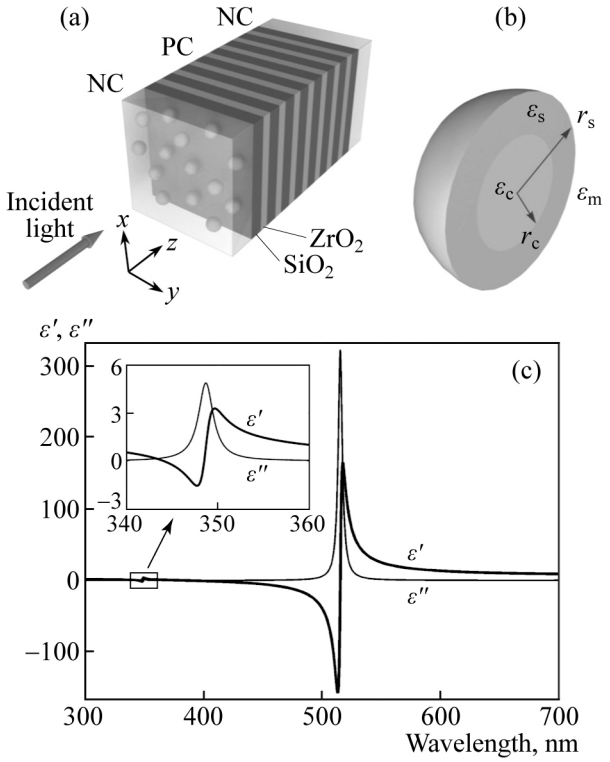

Fig. 1. (a) Schematic view of a one-dimensional photonic crystal bounded by nanocomposite layers, (b) nanoparticle cross section, and (c) effective permittivity of the nanocomposite. Parameters: $f = 0.3$, $r_c/r_s = 0.3$, $\varepsilon_m = 2.56$, and $\varepsilon_c = 3$.

The effective permittivity of the nanocomposite is defined by the Maxwell–Garnett formula

$$\varepsilon = \varepsilon_m\left(1 + \frac{3f\alpha}{1 - f\alpha}\right), \tag{1}$$

where f is the filling factor, i.e., the volume fraction of nanoparticles in the composite. The parameter α is proportional to the dipole polarizability of the layered nanoparticle. For a spherical particle with the core permittivity ε_c and the shell permittivity ε_s in a medium with the permittivity ε_m this parameter is defined by the expression [14, 15]

$$\alpha = \frac{(\varepsilon_s - \varepsilon_m)(\varepsilon_c + 2\varepsilon_s) + \beta(\varepsilon_m + 2\varepsilon_s)(\varepsilon_c - \varepsilon_s)}{(\varepsilon_s + 2\varepsilon_m)(\varepsilon_c + 2\varepsilon_s) + 2\beta(\varepsilon_s - \varepsilon_m)(\varepsilon_c - \varepsilon_s)}, \tag{2}$$

where $\beta = (r_c/r_s)^3$ is the ratio of the particle core volume to the total particle volume (Fig. 1(b)). In the structure under consideration, nanoparticles consist of a dielectric core with the permittivity $\varepsilon_c = 3$ and a silver shell with the permittivity ε_s expressed by the Drude–Sommerfeld formula [14, 15]

$$\varepsilon_s(\omega) = \varepsilon_0 - \frac{\omega_p^2}{\omega(\omega + i\gamma)}, \tag{3}$$

where ε_0 is the constant to allow for contributions from interband transitions of bound electrons, ω_p is the plasma frequency, γ is the damping factor (the inverse of the electron relaxation time), and ω is the incident light frequency. For silver, $\varepsilon_0 = 5$, $\hbar\omega_p = 9$ eV, and $\hbar\gamma = 0.02$ eV.

Figure 1(c) shows calculated dependence of the effective NC permittivity on the incident light wavelength for our chosen parameters of the nanocomposite. It is evident from the figure that there arise two, shortwave and longwave, resonant parts of the permittivity, which are related in nature to the plasmon resonance of the nanoparticles. An increase in the core permittivity results in increasing shortwave resonant part of the permittivity, while its longwave part decreases. As the matrix permittivity increases, the situation is reverse. In addition, both resonances redshift. A decrease in the shell thickness results in enhanced coupling of plasmons localized at the shell boundaries, and the shortwave resonant part of the permittivity is seen to blueshift while the longwave part redshifts. When the real part of the NC permittivity becomes negative, the NC becomes similar to a metal mirror.

3. RESULTS OF CALCULATIONS

Figure 2(a) shows the dependence of the structure transmission spectrum on the thickness d of the first SiO_2 layer immediately adjacent to the NC layer. Two transmission peaks are seen near the shortwave boundary of the PC BG. As was shown in [16], these peaks correspond to coupled TPPs. The light field at the wavelength of these peaks is localized at the interface between the PC and NC layers and exponentially decays through the depth of the superlattice and the composite. In fact, the light turns out to be between two mirrors, the Bragg and the metal ones, because the OTS wavelength falls within the bandgap of the photonic crystal and is also in the region of negative values of the real part of the NC permittivity. Figure 2(b) shows wavelength repulsion of the peaks corresponding to the coupled TPPs.

It is evident from Fig. 2 that the positions of the peaks and distances between them appreciably vary with the first-layer thickness d. The peak splitting is due to removal of degeneracy that arises from the coupling of the optical Tamm modes localized at the interface. As was pointed out in [17], the increase in the thickness of the first PC layer immediately adjacent to the plasma-like medium (in our case it is the NC with the negative real part of its permittivity in this wavelength range) entails an increase in the OTS wavelength (shown by dots in the figure) and thus a change in the wavelength of the OTS localized at the interface of the NC and the layer of variable thickness.

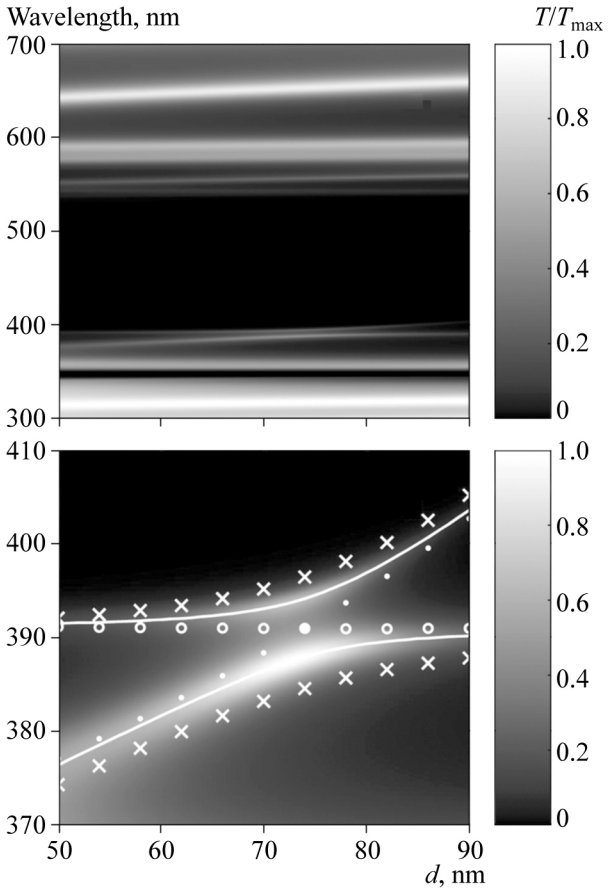

Fig. 2. (a) Calculated system transmission spectrum as a function of the first SiO_2 layer thickness d at normal incidence of light ($T_{max} = 0.9144$) and (b) scaled-up motion of the peaks corresponding to the Tamm plasmon polaritons ($T_{max} = 0.4124$). Maxima of transmission peaks are shown for the number of PC layers $N = 17$ (solid curve) and $N = 13$ (×). Dots and circles show the OTS positions for the NC–PC and PC–NC structures respectively. Parameters: $f = 0.3$, $r_c/r_s = 0.3$, $\varepsilon_m = 2.56$, and $\varepsilon_c = 3$.

The wavelength of the second OTS localized at the other PC interface does not change (shown by circles in the figure). Wavelength tuning of the coupled OTS modes results in increasing distance between the peaks. This behavior of the dispersion curves is called quasi-intersection. The distance between the peaks reaches the minimum at $d = 74$ nm, i.e., when the structure becomes symmetric and the wavelengths of the coupled Tamm modes coincide, their dispersion curves intersect.

Considerable dependence of the transmission peak positions on the thickness of the first PC layer opens up a possibility of developing a tunable filter on the basis of a similar structure. To this end, the first layer should be shaped as a sharp wedge. The boundaries of the layer stop being plane parallel, but the one-dimensional approximation will remain valid if an appropriate optical beam aperture is chosen.

When the number of the PC layers decreases, the wavelength distance between the peaks corresponding to the coupled TPPs increases (splitting increases). This is because the distance between the NC layers decreases and the spatial overlapping region of coupled Tamm modes increases, which leads to stronger coupling of the modes and splitting of the peaks (see Fig. 2(b)).

Figure 3(a) depicts behavior of peaks corresponding to coupled TPPs with varying angle of incidence of s-polarized light on the structure. The wavelengths of the OTSs independently excited on both PC–NC interfaces coincide; therefore, no quasi-intersection is observed. As the angle of incidence of light increases, the wavelength of each coupled OTS decreases, which leads to a decrease in the wavelengths corresponding to the split peaks. As the angle of incidence increases, the field at the OTS wavelength faster decays through the PC depth, and the spatial overlapping region of interacting Tamm modes decreases, which results in their weaker coupling and a decrease in the peak splitting. They asymptotically approach the wavelength of uncoupled OTS: degeneracy of the states decreases. Crosses in the figure show that the distance between the peaks increases with decreasing number of PC layers.

There are technologies for production of nanoparticles that allow varying the core and shell size in a wide range [15]. This opens up an additional possibility of tuning transmission peak positions during the production of these structures. Figure 3(b) shows motion of peaks as the ratio r_c/r_s increases. It is evident from the figure that the peaks redshift. This is because the NC permittivity has two resonant regions corresponding to two surface plasmons localized in the particle at two interfaces of the metal shell with the core and the matrix (see Fig. 1(c)). In our calculations a stronger longwave resonance corresponding to the outer boundary is manifested. As the thickness of the shell decreases, the coupling of the plasmons localized on its boundaries becomes stronger, and mode repulsion is observed, that is, the shortwave edge of the resonant region of the permittivity moves towards shorter wavelengths and the longwave edges moves towards longer wavelengths. Therefore, the region of negative values of the real part of the NC permittivity redshifts, as also does the wavelength of the OTSs localized at the PC edges (shown by dots in the figure). The mechanism for the decrease in the splitting of the peaks corresponding to the coupled TPPs is the same as for the increase in the angle of incidence of light, being connected with the sharper decay of the field through the depth of the structure at the OTS wavelength.

Figures 3(c,d) show the motion of the peaks as a function of the nanoparticle core and nanocomposite

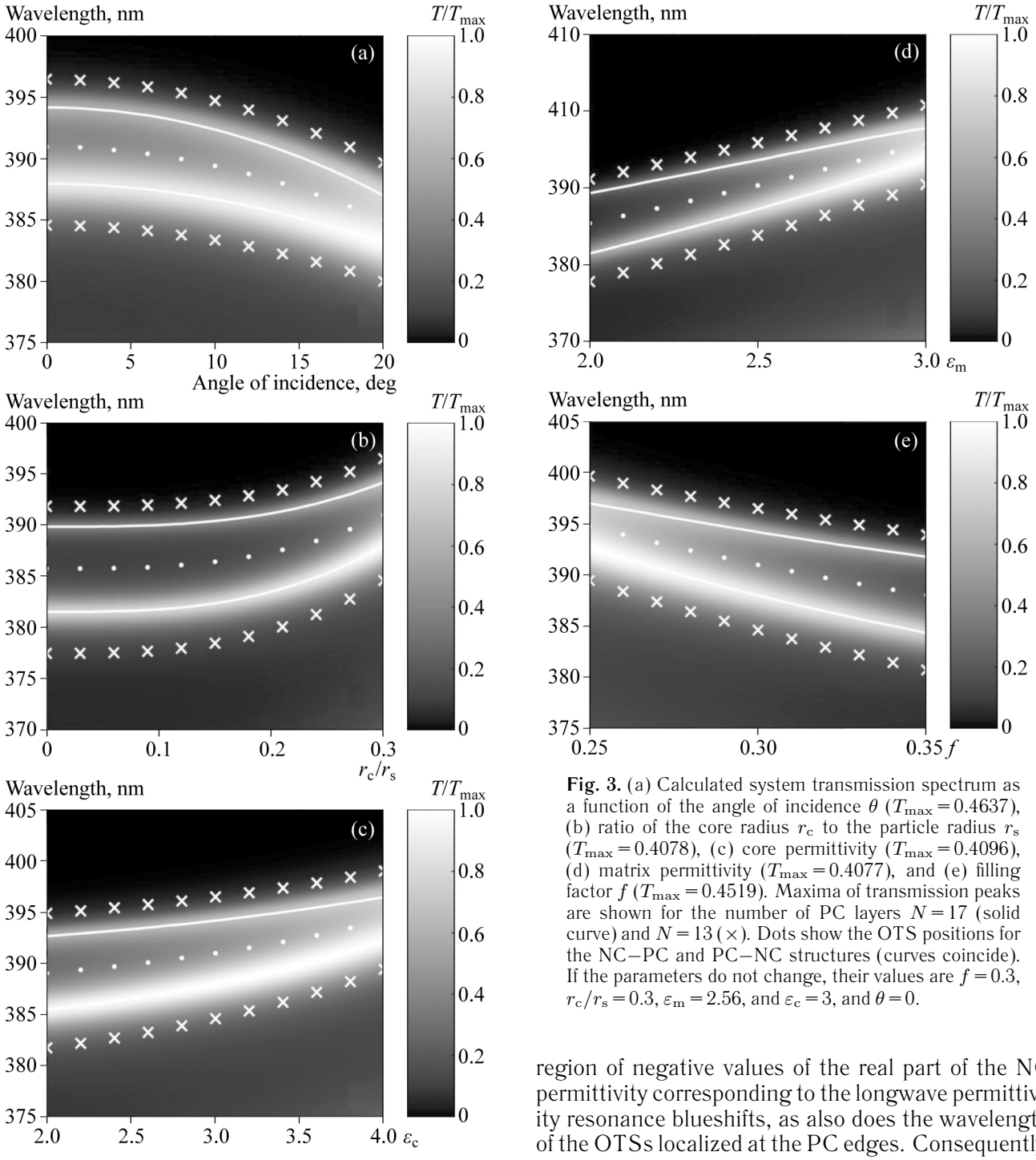

Fig. 3. (a) Calculated system transmission spectrum as a function of the angle of incidence θ ($T_{max} = 0.4637$), (b) ratio of the core radius r_c to the particle radius r_s ($T_{max} = 0.4078$), (c) core permittivity ($T_{max} = 0.4096$), (d) matrix permittivity ($T_{max} = 0.4077$), and (e) filling factor f ($T_{max} = 0.4519$). Maxima of transmission peaks are shown for the number of PC layers $N = 17$ (solid curve) and $N = 13$ ($\times$). Dots show the OTS positions for the NC–PC and PC–NC structures (curves coincide). If the parameters do not change, their values are $f = 0.3$, $r_c/r_s = 0.3$, $\varepsilon_m = 2.56$, and $\varepsilon_c = 3$, and $\theta = 0$.

matrix permittivity. As the permittivity of the core and the matrix increases, both resonances of the NC permittivity redshift. Therefore, the region of negative values of the real part of the NC permittivity also redshifts, as also does the wavelength of the OTSs localized at the PC edges. The mechanism for the decrease in the peak splitting is the same as in Fig. 3(a).

The peak positions can also be controlled by varying the filling factor f (Fig. 3(e)). As f increases, the region of negative values of the real part of the NC permittivity corresponding to the longwave permittivity resonance blueshifts, as also does the wavelength of the OTSs localized at the PC edges. Consequently, the split peaks also blueshift. The field decay at the OTS wavelength through the PC depth becomes slow, and the spatial overlapping region of the interacting Tamm modes increases, which leads to their stronger coupling and higher peak repulsion.

4. CONCLUSIONS

Spectral properties of a one-dimensional photonic crystal bounded by nanocomposite layers of nanopar-

ticles with a dielectric core and a metal shell are theoretically studied.

It is shown that positions of split transmission peaks corresponding to coupled Tamm plasmon polaritons can be controlled by varying the nanocomposite parameters.

The dependence of the positions of the split peaks on the thickness of the first layer of the photonic crystal and on the angle of incidence can help in development of tunable filters based on this structure.

ACKNOWLEDGEMENTS

The work was supported by the Siberian Branch of the Russian Academy of Sciences, Project II.2P (0358-2015-0010); Scholarship of the President of the Russian Federation SP-227.2016.5; RFBR and Government of the Krasnoyarsk Territory, Krasnoyarsk Region Science and Technology Support Fund, Projects 16-42-243065 and 17-42-240464.

REFERENCES

1. A.P. Vinogradov, A.V. Dorofeenko, A.M. Merzlikin, and A.A. Lisyansky, "Surface States in Photonic Crystals," Phys. Usp. **53**, 243 (2010).
2. A. Kavokin, I. Shelykh, and G. Malpuech, "Optical Tamm States for the Fabrication of Polariton Lasers," Appl. Phys. Lett. **87**, 261105 (2005).
3. A.V. Kavokin, I.A. Shelykh, and G. Malpuech, "Lossless Interface Modes at the Boundary between Two Periodic Dielectric Structures," Phys. Rev. B. **72**, 233102 (2005).
4. M. Kaliteevski, I. Iorsh, S. Brand, R.A. Abram, J.M. Chamberlain, A.V. Kavokin, and I.A. Shelykh, "Tamm Plasmon-Polaritons: Possible Electromagnetic States at the Interface of a Metal and a Dielectric Bragg Mirror," Phys. Rev. B. **76**, 165415 (2007).
5. S.Ya. Vetrov, R.G. Bikbaev, and I.V. Timofeev, "Optical Tamm States at the Interface between a Photonic Crystal and a Nanocomposite with Resonance Dispersion," JETP. **117**, 988 (2013).
6. M. Sasin, R. Seisyan, M. Kalitteevski, S. Brand, R. Abram, J. Chamberlain, A.Yu. Egorov, A.P. Vasil'ev, V.S. Mikhrin, and A.V. Kavokin, "Tamm Plasmon Polaritons: Slow and Spatially Compact Light," Appl. Phys. Lett. **92**, 251112 (2008).
7. T. Goto, A.V. Dorofeenko, A.M. Merzlikin, A.V. Baryshev, A.P. Vinogradov, M. Inoue, A.A. Lisyansky, and A.B. Granovsky, "Optical Tamm States in One-Dimensional Magnetophotonic Structures," Phys. Rev. Lett. **101**, 113902 (2008).
8. W.L. Zhang and S.F. Yu, "Bistable Switching Using an Optical Tamm Cavity with a Kerr Medium," Opt. Commun. **283**, 2622 (2010).
9. H. Zhou, G. Yang, K. Wang, H. Long, and P. Lu, "Multiple Optical Tamm States at a Metal–Dielectric Mirror Interface," Opt. Lett. **35**, 4112 (2010).
10. A.P. Vinogradov, A.V. Dorofeenko, S.G. Erokhin, M. Inoue, A.A. Lisyansky, A.M. Merzlikin, and A.B. Granovsky, "Surface State Peculiarities in One-Dimensional Photonic Crystal Interfaces," Phys. Rev. B. **74**, 045128 (2006).
11. X.-L. Zhang, J.-F. Song, X.-B. Li, J. Feng, and H.-B. Sun, "Optical Tamm States Enhanced Broad-Band Absorption of Organic Solar Cells," Appl. Phys. Lett. **101**, 243901 (2012).
12. Y. Gong, X. Liu, H. Lu, L. Wang, and G. Wang, "Perfect Absorber Supported by Optical Tamm States in Plasmonic Waveguide," Opt. Exp. **19**, 18393 (2011).
13. I. Iorsh, P.V. Panicheva, I.A. Slovinskii, and M.A. Kaliteevskii, "Coupled Tamm Plasmons," Tech. Phys. Lett. **38**(4), 351 (2012).
14. A. Sihvola, *Electromagnetic Mixing Formulas and Applications* (Institution of Engineering and Technology, London, 2008).
15. N.N. Beletskii, S.A. Borysenko, and N.I. Gvozdev, "Interaction of Plasma and Defective Modes in One-Dimensional Layered Periodic Dielectric Structures Bordering Upon Plasma-Like Media," Radiophys. Electron. **4**(3), 55 (2013).
16. V. Klimov, *Nanoplasmonics* (CRC Press, Boca Raton, 2014).
17. S.Ya. Vetrov, P.S. Pankin, and I.V. Timofeev, "Spectral Properties of a Photonic Crystal Conjugated to Nanocomposite Containing Shell Particles," Memoirs of the Faculty of Physics, Lomonosov Moscow State Univ. N 4, 154315 (2015).